

Proteomic study of hepatic apoptosis induced by overexpression of GOS2

Yaxin Qiu

Shandong Provincial Hospital Affiliated to Shandong First Medical University

Xiaoming Zhou

Shandong Provincial Hospital Affiliated to Shandong First Medical University

Zhenyuan Zhang

Shandong Provincial Hospital Affiliated to Shandong First Medical University

Wenxiu Sun

Department of Nursing, Taishan Vocational College of Nursing

Shizhan Ma (✉ msz2010lw@163.com)

Shandong Provincial Hospital Affiliated to Shandong First Medical University

Research Article

Keywords: GOS2, Apoptosis, Proteomics analysis

Posted Date: March 29th, 2022

DOI: <https://doi.org/10.21203/rs.3.rs-1342968/v1>

License:  This work is licensed under a Creative Commons Attribution 4.0 International License.

[Read Full License](#)

Abstract

Background: G0S2 was initially identified in blood mononuclear cells after the induction of cell cycle progression. The translation of G0S2 produces a small basic protein 103 amino acids in length. Initially, G0S2 was thought to mediate re-entry into the cell cycle by promoting the transition from the G0 to the G1 phase. Recent studies have identified roles for G0S2 in cancer, inflammation, and various metabolic processes. In lipid metabolism, G0S2 binds to ATGL and inhibits lipolysis. G0S2 also binds specifically to BCL-2 and inhibits the formation of the antiapoptotic body BCL-2/Bax, which in turn favors apoptosis. Whether there are other mechanisms and the proteins involved in these processes are not known; therefore, we used proteomics to identify differentially expressed proteins related to G0S2.

Methods: G0S2-overexpressing adenovirus was injected into C57/BJL mice, the livers were collected, and proteins were identified by mass spectrometry. The identified proteins were analyzed by Gene Ontology (GO) and KEGG.

Results: In total, 3765 liver proteins were identified, of which 3745 were quantified. The expression of 320 proteins was found to be upregulated, and that of 101 proteins was downregulated. These results indicated that G0S2 overexpression significantly altered the proteomic profile. There were 63 differential proteins involved in apoptosis, of which 45 were up-regulated and 18 were down-regulated.

Conclusion: Our preliminary study showed that G0S2 overexpression in the liver led to specific protein spectrum changes, with 63 differentially expressed proteins involved in the regulation of apoptosis, elucidating an important relationship between G0S2 and apoptosis. This finding indicated that G0S2 may involve in cancer, neurodegenerative diseases and numerous metabolic diseases as an apoptotic factor, providing new insights into the mechanisms of disease development.

Introduction:

G0/G1 switch gene 2 (G0S2) was first identified in blood single-nucleated cells (PBMCs). During the drug-induced cell cycle transition from the G0 to the G1 phase, the gene is differentially expressed. The G0S2 gene codes for a small protein of 103 amino acids that is found only in spinal animals and is highly conserved among species. It shows 78% homology in humans and mice. Based on protein secondary structure predictions, it has been proposed that the G0S2 protein contains two α -helices separated by hydrophobic sequences that have the potential to produce turns and exhibit a β -sheet conformation^[1]. The promoter region of G0S2 contains potential binding sites for the transcription factors AP1, AP2, AP3, and nuclear factor of activated T cells (NFAT), and a number of sequence motifs are responsive to the transcriptional activation of specific lectins, retinoids (RA), peroxisome proliferator-activated receptor agonists (PPARs), glucose, and insulin. Thus, G0S2 is a multifaceted protein involved in proliferation, apoptosis, inflammation, metabolism, and cancer. G0S2 is highly expressed mainly in white, brown adipose tissues and the liver^[2] and has been shown to localize to different organelles, including mitochondria, the endoplasmic reticulum, and lipid droplets. G0S2 is involved in cellular pathology mainly

through protein–protein interactions and physiological processes. Most notably, G0S2 specifically interacts with adipose triglyceride lipase, inhibiting its activity and leading to inhibited lipolysis.^[2] Similarly, G0S2 binds to BCL-2 and inhibits the formation of BCL2/Bax pro-apoptotic vesicles, which in turn promotes apoptosis.^[3] Furthermore, in terms of cell proliferation, G0S2 interacts directly with nucleolin to mediate intracellular retention of nucleoli, which in turn inhibits the proliferation of hematopoietic stem cells^[4]; during CKD development, G0S2 interacts with the P65 protein to promote nuclear localization of P65, which in turn promotes inflammation^[5].

Apoptosis is an important component of the cell development process, and inappropriate apoptosis is a major factor. In the development of human diseases, such as metabolic diseases, autoimmune diseases, inflammation and cancer. The role of G0S2 in apoptosis is poorly understood and to investigate the role of G0S2 in apoptosis, we used proteomics, GO analysis and KEGG analysis to compare differences in protein expression in G0S2-overexpressing mice and wild-type mice. We found that the expression of many apoptosis-related proteins was up- or downregulated, which may enable a search for new therapeutic targets for diseases related to metabolic diseases, inflammation and cancer.

Methods:

Animals: Eight-week-old male C57BL/6 mice were utilized in this study. They were kept separately under regulated light/dark (12/12 h) and temperature (25°C) conditions. The mice had unlimited access to water and food^[6]. Every three days, the mice were fed new chow and their weight increase was measured on a seven-day cycle. A dose of Ad-LacZ (4.5×10^{10} PFU/ml) or Ad-G0S2 (2.51×10^{10} PFU/ml) was administered through the tail vein after 5 weeks of feeding. A dose of Ad-LacZ or Ad-G0S2 was administered after 5 weeks of feeding. Mice in the experimental group were denied food for 16 hours before to death, although they were free to consume water at their leisure. All procedures were carried out under anesthesia using sodium pentobarbital in order to decrease discomfort. And their livers were quickly removed and frozen in liquid nitrogen in preparation for further investigation. Finally, these mice were euthanized by cervical dislocation. The experimental procedure was approved by the Animal Ethics.

Protein extraction and digestion

The SDT buffer (4% SDS, 100 mM Tris-HCl, and 1 mM DTT, pH 7.6) was utilized for sample lysis and protein extraction, and the results were positive. The quantity of protein in the sample was determined using a BCA Protein Assay Kit (Bio-Rad, United States). The filter-aided sample preparation (FASP) approach established by Matthias Mann was used to carry out the trypsin digestion of the proteins. The digested peptides in each sample were desalted on C18 cartridges (Empore™ SPE Cartridges C18 (standard density), bed I.D. 7 mm, volume 3 ml, Sigma), concentrated by vacuum centrifugation and reconstituted in 40 µl of 0.1% (v/v) formic acid^[7].

SDS–PAGE

For each sample, 20 micrograms of protein were combined with 5X loading buffer and then cooked for 5 minutes. The proteins were separated on a 12.5% SDS-PAGE gel to get their final size (a constant current of 14 mA was applied for 90 min). The presence of protein bands was identified using Coomassie Blue R-250 staining.

LC-MS/MS analysis

This investigation was carried out using a timsTOF Pro mass spectrometer (Bruker), which was paired to a nanoElute HPLC system from Bruker Daltonics, for periods of 60, 120, and 240 minutes each time. In buffer A (0.1% formic acid), the peptides were loaded onto a reversed-phase trap column (Thermo Scientific Acclaim PepMap100, 100 μm *2 cm, nanoViper C18) that was connected to a reversed-phase C18 analytical column (Thermo Scientific Easy Column, 10 cm long with a 75 μm inner diameter and 3 μm diameter resin) and separated using a linear gradient of buffer B (84% acetonitrile and 0.1% formic acid). The positive ion mode of the mass spectrometer was used for this experiment^[8]. In addition, ion mobility MS spectra were obtained across a mass range of m/z 100–1700 and 1/k0 of 0.6 to 1.6, and then 10 cycles of PASEF MS/MS were done with a target intensity of 1.5k and a threshold of 2500 were performed on the data acquired. It was decided to enable active exclusion with a release time of 0.4 minutes.

Identification and quantitation of proteins

The library identification and quantitative analysis were carried out using the MaxQuant program (version 1.6.14)^[9]. An first search was conducted using a precursor mass window of 6 ppm. MS data were searched against SwissProt_Mus_musculus_17063_20210106 in Fasta. In the search, trypsin was used as the primary enzymatic enzyme, and the maximum number of miss-cleavage sites was set at two, while the fragment ion mass tolerance was set at 20 ppm^[10].

Protein N-terminal acetylation and methionine oxidation were both characterized as variable modifications for the sake of database searching, but carbamidomethylation of cysteines was considered a fixed modification. It was decided that a 0.01 false discovery rate (FDR) limit should be used for peptide and protein identification. The adjusted spectral protein intensity (LFQ intensity) was used to determine the amount of proteins in the sample. Proteins with a fold change > 2 or < 0.5 and p value (Student's t test) < 0.05 were considered differentially expressed proteins.

Bioinformatics analysis

We utilized the Cluster 3.0 program (<http://bonsai.hgc.jp/mdehoon/software/cluster/software.htm>) and the Java Treeview software (<http://jtreeview.sourceforge.net>) to conduct hierarchical cluster analysis on the phosphorylated peptides^[11]. Several algorithms were considered for hierarchical clustering, including the Euclidean distance method for the similarity measure and the average linkage clustering algorithm (which clusters observations based on their centroids) for clustering. A heatmap is often used in conjunction with a dendrogram to provide extra visual assistance.

GO annotation

Finding homologous sequences among the protein sequences of the differentially expressed proteins was accomplished using local searches with the NCBI BLAST + client program (ncbi-blast-2.2.28+win32.exe) and InterProScan, which is available for free download from the NCBI website^[12]. Then, using the software application Blast2GO, gene ontology (GO) concepts were mapped to the sequences and the sequences were annotated. The results of the GO annotation were visualized using R scripts.

KEGG annotation

To get their KEGG or Gene Ontology identifications, the investigated proteins were BLASTed against the online Kyoto Encyclopedia of Genes and Genomes (KEGG) database (<http://geneontology.org/>) and then mapped to KEGG pathways, as previously described^[13].

Enrichment analysis

The Fisher's exact test was used to do the enrichment analysis, with the assumption that all measured proteins were included in the background dataset. The Benjamini–Hochberg correction for multiple testing was used to alter the p values that were calculated. We only included relevant functional categories and pathways with p values below 0.05, which was the cutoff point for statistical significance^[14].

TUNEL staining and immunohistochemical staining

TUNEL staining and immunohistochemistry (IHC) were performed on mouse liver tissues that had been fixed in 4% paraformaldehyde and examined under a light microscope^[15]. TUNEL labeling was performed on sections using an in situ cell death detection kit (Servicebio G1501) to identify cell death in situ (positive apoptotic cells were green). Sections were submerged in citrate buffer for 10 minutes before being autoclaved at 120°C for 10 minutes and then immersed in 3% hydrogen peroxide (H₂O₂). Sections were incubated with the following primary antibodies: FADD(cat. no. ab124812, Abcam), Bax (cat. no. ab32503, Abcam), Caspase3(cat. no. ab184787, Abcam), ROCK1(cat.no. ab134181, Abcam), Bad(cat. no. ab32445, Abcam), NACA(cat. no. A10122, Abclonal), at 4°C overnight. The sections were incubated with HRP-labeled secondary antibody for 50 min at room temperature^[16]. Finally, DAB staining solution was added, and a brownish yellow color indicated positive expression; then, the nuclei of the cells were re-stained with hematoxylin violet, which showed a blue color.

Results:

Quantitative proteomic analysis: Proteome changes in the G0S2 overexpression group and control group were analyzed by LC–MS/MS. A total of 3765 proteins were identified, of which 3745 proteins were quantified. To further understand their functions, all identified proteins were annotated according to different categories, including GO terms, KEGG pathways and PPIs.

Evaluation of G0S2 overexpression in mouse hepatic proteomics: Among the quantifiable protein genes, the expression of 320 proteins was found to be upregulated, and that of 101 proteins was downregulated (Fig. 1). This finding indicated that G0S2 overexpression significantly altered the proteomic profile. Among the identified proteins, 63 differentially expressed proteins were involved in apoptosis, the expression of 45 proteins was upregulated, and that of 18 proteins was downregulated (Fig. 2). A list of 421 apoptosis associated proteins with their fold changes are shown in supplementary file.

Bioinformatics analysis of protein function and subcellular localization after G0S2

overexpression: Through GO analysis, we analyzed the role of G0S2 in the apoptosis in terms of biological process, cellular component and molecular function categories. In terms of biological processes, 316 proteins were involved in the cellular processes of single organisms, 197 proteins were involved in the metabolic processes of organic nitrogen compounds, 171 proteins were involved in the metabolic processes of single organisms, 102 proteins were involved in the establishment of cellular localization, 97 proteins were involved in small-molecule metabolic processes, 91 proteins were involved in intracellular transport, 86 proteins were involved in nitrogen compound transport, 86 proteins were involved in protein localization, 78 proteins were involved in amide transport, 78 proteins were involved in peptide transport, and 63 proteins were involved in apoptotic processes (Fig. 3). In terms of molecular function (Fig. 4), 18% of the proteins were associated with protein binding, and 13% proteins were involved with enzyme binding, which may indicate that G0S2 is involved in apoptosis through protein-protein or enzyme binding. In terms of cellular components (Fig. 5), 77% of the proteins were in the cytoplasm, and 8% were in membrane-bound organelles (e.g., mitochondria and the endoplasmic reticulum), and G0S2 is a mitochondrial protein, which is consistent with our study. The KEGG analysis revealed that 14% of the differentially expressed proteins were associated with metabolism (Fig. 6), and according to previously obtained results, these differentially expressed proteins were involved in apoptosis.

We present 63 of the differential proteins in a heatmaps. To further understand the role between these differential proteins, we performed an additional PPI analysis (Figure 7) which revealed multiple apoptosis-related protein interactions, suggesting a complex mechanism of G0S2 action in regulating apoptosis.

TUNEL staining and immunohistochemical staining to verify apoptosis: TUNEL staining showed that apoptotic cells were significantly increased in liver tissues of G0S2-overexpressing mice (Fig. 8), indicating that G0S2 can promote apoptosis. Immunohistochemical staining (Fig. 9) revealed apoptotic markers, and unsurprisingly, the expression of FADD, BAX, Caspase3, and ROCK1 was significantly increased in the liver tissues of G0S2-overexpressing mice, while the expression of BAD and NACA was decreased, which was consistent with previous results. This suggests that G0S2 can lead to apoptosis by promoting increases in the expression of FADD, BAX, Caspase3, and ROCK1 or by promoting decreased expression of BAD and NACA, consistent with our proteomic analysis findings.

Discussion:

Apoptosis is involved in the development of many diseases, such as impaired clearance of apoptotic cells or reduced apoptosis leads to autoimmune diseases and cancer; increased apoptosis leads to neurodegenerative diseases and myocardial infarction; therefore, impaired clearance of apoptotic cells, reduced or increased apoptosis are susceptibility factors for diseases^[17]. In our study, by comparing the liver proteomics of G0S2 overexpressing mice and control mice, we identified 63 differential proteins involved in the apoptotic process. It indicates that the role of G0S2 in the apoptotic process is crucial.

Previous studies have shown that G0S2 mainly binds to BCL-2, interferes with the formation of BCL-2/Bax anti-apoptotic vesicles and promotes Bax release, which in turn promotes apoptosis^[3]. The elevation of Bax found in our study is consistent with previous studies, and it is conjectured that G0S2 can promote Bax expression in addition to interfering with dimer synthesis. And FADD, Caspase3 (an important molecule in the apoptotic pathway) were elevated. FADD, also known as Fas-like death structural domain protein, recruits FADD when external apoptotic signals are activated, which in turn activates the Caspase cascade reaction and induces apoptosis, where Caspase3 is the executor in the cascade reaction. And Toll-like receptor 3(TLR3), promotes apoptosis in cancer cells through an extrinsic pathway that activates caspase8 which in turn activates caspase3^[18]. Thus G0S2 not only acts in the intrinsic apoptotic pathway, but also mediates the extrinsic apoptotic pathway.

Rho-related kinase (ROCK) was initially identified as a serine/threonine kinase (RhoA) that binds to guanosine triphosphate (GTP)^[19]. There are two isoforms of ROCK, including ROCK1 and ROCK2, both of which play a key role in apoptosis. ROCK1 cleavage by caspase-3 during apoptosis^[20]. ROCK1 inhibition reduces apoptosis in cardiomyocytes during ischemia-reperfusion injury, promotes embryonic stem cell survival, and inhibits androgen-induced apoptosis and genotoxic stress-induced cell death in prostate cancer cells^[21]. Elevated ROCK1 expression in liver tissue of AD-G0S2 mice is consistent with G0S2 promoting apoptosis.

The accumulation of reactive oxygen species can induce a caspase cascade reaction, which in turn induces apoptosis^[22]. N-acetylcysteine amide (NACA), acts as a "free radical scavenger" with apoptosis-inhibiting effects^[23]. It has been demonstrated that it inhibits apoptosis through various pathways, such as Upregulating Thioredoxin-1, Inhibiting ASK1/p38MAPK Pathway, Suppressing Oxidative Stress and Nrf2-ARE pathway^[24, 25].

Moreover, G0S2 was found to also sensitize apoptosis induced by the DNA damage response(DDR)^[3], and we found elevated expression levels of MRE11, which plays a coordinating role in the DDR^[26]. Hence, G0S2 overexpression may lead to elevated levels of proteins involved in the DDR. HIP1R is indirectly involved apoptosis. Its overexpression decreases p-AKT and p-mTOR expression, while caspase-9 and Bak activity increase; thus apoptosis can be induced through the PI3K/AKT signaling pathway mediated through Bak. Thus, G0S2 may also be involved in AKT1/mTOR-mediated apoptosis, which has not been investigated.

Of course, there are other apoptotic pathway-related factors, such as SDF2L1, a stromal cell-derived factor and endoplasmic reticulum stress-associated endoplasmic reticulum-resident protein, and endoplasmic reticulum stress upregulates SDF2L1 expression, which may play a negative regulatory role in cancer by activating endoplasmic reticulum stress to balance the cellular environment and promote apoptosis^[27]. TMEM214, a human transmembrane protein 214, has been shown to be a key molecule in endoplasmic reticulum stress-induced apoptosis.

Previous studies have shown that G0S2 is a downstream molecule of the TNF/NF- κ B signaling pathway, and its activation leads to elevated G0S2 expression. We found that NOD1, an NH₂-terminal protein linked to the nucleotide-binding region and containing multiple leucine-rich repeats in the COOH terminus, is an APAF-1-like molecule that regulates both apoptosis and NF- κ B activation pathways^[28]. The relationship between NOD1 and G0S2 was demonstrated by a 20-fold increase in NOD1 expression after G0S2 overexpression, suggesting an important role for G0S2 in the apoptotic pathway of hepatocytes.

G0S2 is an oncogene, and some studies have found that G0S2 is activated by the TNF α -induced NF- κ B signaling pathway, which in turn induces the apoptosis of cancer cells. Moreover, G0S2 contains CpG islands and is highly methylated and epigenetically silenced in human cancer cells, further suggesting that G0S2 is an oncogene.^[3] In cancer, apoptosis is subdivided into the P53-dependent and P53-independent pathways. We found elevated expression levels of many oncogenes, including DNAJA3, which forms a complex with p53 under hypoxic conditions, directing p53 translocation to mitochondria and subsequently initiating the mitochondrial apoptotic pathway^[29]. UBQLN1 negatively regulates mTOR, promotes autophagy, and cleaves P53 to suppress tumorigenesis^[30]. These two factors are involved in the P53-dependent mitochondrial apoptotic pathway. The next step may be investigation into whether G0S2 can execute mitochondrial apoptosis dependent on P53. MYC-dependent cell death is an important pathway of apoptosis in cancer cells. PTGIS is a hypoxia-inducible factor-1 α (HIF-1 α) target gene that inhibits the proliferation of bladder cancer cells and is a tumor suppressor^[31]. IGF2R, also known as M6P/IGF2R, was identified in 1999 as a tumor suppressor gene that inhibits cell proliferation^[32]. FHIF is an oncogene with decreased expression in esophageal cancer. Although there are few reports in the literature, it has been reported that the G0S2 gene inhibits cell proliferation in bladder cancer and lung squamous carcinoma cells^[33, 34] and that ASK1 has antitumor activity, which is consistent with our study. However, in our study, SLC9A3R1 (solute carrier family 9, subfamily A [also known as NHE3, cationic proton reverse transporter protein 3], member 3 regulator 1) is involved in the activation of autophagy and plays a potential antitumor role in breast cancer^[35], suggesting that G0S2 may play a tumor suppressive role in breast cancer.

In addition, many molecules are involved in the PI3K/AKT1/mTOR signaling pathway, e.g., Deptor, an inhibitory subunit of mTORC1/mTORC2. When mTORC1/mTORC2 activity is reduced, Deptor is recruited to further repress mTORC1/mTORC2 expression. Activated mTORC1/mTORC2 directly phosphorylates Deptor, decreasing its inhibitory effect and further activating mTORC1/mTORC2 signaling. mTOR is an important eukaryotic signaling molecule whose stability affects cytokine expression in T cells,

participates in immunosuppression, influences transcription and protein synthesis, and regulates cell growth, apoptosis, autophagy, etc. Thus, G0S2 may also be involved in the AKT1/mTOR signaling pathway, which regulates apoptosis. However, no literature has been published to verify this supposition.

Our study found that G0S2 mediates apoptosis of cancer cells but also participates in the apoptosis of neuronal cells, and one study demonstrated that PCMT1 reduced MST1-induced apoptosis of neuronal cells after subarachnoid hemorrhage (SAH) in rats. It shows promise as a therapeutic for early brain injury after subarachnoid hemorrhage^[36]. UBQLN1 protects against oxidative stress and ischemia-induced neuronal injury by promoting the clearance of damaged proteins. It is closely associated with the development of neurodegenerative diseases such as Alzheimer's disease and Huntington's disease. Thus, UBQLN1 has a proapoptotic effect, and UBQLN1 is associated with the development of epilepsy^[30, 37], suggesting that G0S2 is closely associated with the development of neurodegenerative diseases and may be a hotspot of future research.

In addition, we found that the expression of factors involved in other forms of cell death was elevated after overexpression of G0S2. For example, RIPK1/3, a receptor-associated protein kinase, mediates cell necrosis in the absence of apoptotic conditions. The expression of both RIPK1/3 was elevated after G0S2 overexpression, suggesting that G0S2 also mediates programmed cell necrosis. The expression levels of HMOX1 heme oxygenase 1, involved in the onset of iron death, were significantly elevated in an iron death model, and the use of HMOX1 inhibitors significantly delayed the onset and progression of iron-related cell death^[38]. G0S2 is also involved in autophagy, iron-related cell death, and programmed cell necrosis. We verified these findings with immunohistochemistry and found that G0S2 overexpression was followed by the elevated expression of FADD, BAX, Caspase3, and ROCK1 and decreased expression of BAD and NACA, consistent with the proteomic results. However, no specific mechanisms or clear signaling pathways were investigated, only providing directions for future research.

Conclusion:

Through our proteomic studies, we found that G0S2 plays a key role in apoptosis and is involved in the development of diseases closely related to apoptosis, such as cancer, metabolic diseases, immune diseases and neurodegenerative diseases, but G0S2 regulation of apoptosis may lead to opposite results, which may be related to the different roles played by G0S2 in different tissues and may be determined by the cellular environment. G0S2 regulates apoptosis through different signaling pathways, such as classical endogenous and exogenous apoptotic pathways, the mitochondrial pathway, the endoplasmic reticulum stress pathway, NF- κ B, and AKT1/mTOR. G0S2 is also involved in autophagy, programmed cell necrosis, the iron-related cell death process, and other forms of cell death by interacting with inflammatory factors. We found an increase in apoptotic cells, an increase in proapoptotic molecules and a decrease in antiapoptotic factors in the liver tissues of G0S2-overexpressing mice. This study provides a direction for future exploration of G0S2 and apoptosis.

Abbreviations:

G0S2, G0/G1 switch gene 2; GO, Gene Ontology; KEGG, Kyoto Encyclopedia of Genes and Genomes; PBMCs, blood single-nucleated cells; NFAT, nuclear factor of activated T cells; RA, retinoids; PPARs, peroxisome proliferator-activated receptor agonists; BCL-2, B cell lymphoma/leukemia-2; Bax, BCL2-Associated X; CKD, Chronic kidney disease; PPI, Protein–protein interaction; FADD, Fas-associating protein with a novel death domain; ROCK, Rho-related kinase; NACA, N-acetylcysteine amide; BAD, B lymphocytoma-2 gene associated promoter; TLR3, Toll-like receptor 3; DDR, DNA damage response; HIP1R, Huntingtin-interacting protein 1-related protein; AKT, Protein Kinase B; SDF2L1, SDF2-like protein 1; TMEM214, Transmembrane Protein 214; TNF, Tumor Necrosis Factor; NF- κ B, Tumor Necrosis Factor; NOD1, Nucleotide-binding oligomerization domain 1; UBQLN1, Ubiquilin 1; mTOR, mammalian target of rapamycin; HIF-1 α , hypoxia-inducible factor-1 α ; IGF2R, IGF2 receptor; SLC9A3R1, solute carrier family 9, subfamily A (also known as NHE3, cationic proton reverse transporter protein 3), member 3 regulator 1); DEPTOR, DEP domain-containing mechanistic target of rapamycin (mTOR)-interacting protein; PCTM1, Protein-L-isoaspartate (D-aspartate) O-methyltransferase 1; SAH, subarachnoid hemorrhage; RIPK, receptor interacting protein kinases; HMOX1, Heme oxygenase 1.

Declarations:

Ethics approval and consent to participate

All methods are implemented in conformity with relative instructions and regulations. All surgeries were performed under sodium pentobarbital anesthesia to minimize pain. The present study was approved by the Ethics Committee of Shandong Provincial Hospital (NSFC:NO.2019-131). All methods were performed following the ARRIVE guidelines.

Consent for publication

Not applicable.

Availability of data and materials

All data generated and analyzed in our study are included in the article and are available in a supplementary file.

Competing interests

The authors declare that they have no competing interests.

Funding

This study was supported by the National Natural Science Foundation of China (grant number 81900716) and Jinan Municipal Science and Technology Project (grant no. 202019091).

Authors' contributions

Y.X.Q and X.M.Z was the experimental designer and executor of the experimental study, completed the data analysis, and wrote the first draft of the paper; S.Z.M was the conceptualizer and leader of the project, and directed the experimental design, data analysis, and paper writing and revision. Z.Y.Z and W.X.S contributed to experiment and data analyze. All authors read and agreed to the final text.

Acknowledgements

Not applicable.

References:

1. Heckmann B L, Zhang X, Xie X, et al. The G0/G1 switch gene 2 (G0S2): regulating metabolism and beyond[J]. *Biochim Biophys Acta*, 2013, 1831(2): 276–81.
2. Yang X, Lu X, Lombes M, et al. The G(0)/G(1) switch gene 2 regulates adipose lipolysis through association with adipose triglyceride lipase[J]. *Cell Metab*, 2010, 11(3): 194–205.
3. Welch C, Santra M K, El-Assaad W, et al. Identification of a protein, G0S2, that lacks Bcl-2 homology domains and interacts with and antagonizes Bcl-2[J]. *Cancer Res*, 2009, 69(17): 6782–9.
4. Yamada T, Park C S, Burns A, et al. The cytosolic protein G0S2 maintains quiescence in hematopoietic stem cells[J]. *PLoS One*, 2012, 7(5): e38280.
5. Matsunaga N, Ikeda E, Kakimoto K, et al. Inhibition of G0/G1 Switch 2 Ameliorates Renal Inflammation in Chronic Kidney Disease[J]. *EBioMedicine*, 2016, 13: 262–273.
6. Young J W, Meves J M, Tarantino I S, et al. Delayed procedural learning in alpha7-nicotinic acetylcholine receptor knockout mice[J]. *Genes Brain Behav*, 2011, 10(7): 720–33.
7. Wang L, Huang Y, Wang X, et al. Label-Free LC-MS/MS Proteomics Analyses Reveal Proteomic Changes Accompanying MSTN KO in C2C12 Cells[J]. *Biomed Res Int*, 2019, 2019: 7052456.
8. Zhao Y, Huang J, Cao J, et al. 4-NBT, a specific inhibitor of Babesia microti thioredoxin reductase, affects parasite biochemistry and proteomic properties[J]. *Ticks Tick Borne Dis*, 2019, 10(5): 1018–1027.
9. Cox J, Mann M. MaxQuant enables high peptide identification rates, individualized p.p.b.-range mass accuracies and proteome-wide protein quantification[J]. *Nature Biotechnology*, 2008, 26(12): 1367–1372.
10. Pachi F, Ruprecht B, Lemeer S, et al. Characterization of a high field Orbitrap mass spectrometer for proteome analysis[J]. *Proteomics*, 2013, 13(17): 2552–62.
11. Roumeliotis T I, Halabalaki M, Alexi X, et al. Pharmacoproteomic study of the natural product Ebenfuran III in DU-145 prostate cancer cells: the quantitative and temporal interrogation of chemically induced cell death at the protein level[J]. *J Proteome Res*, 2013, 12(4): 1591–603.

12. Liu P, Guo L, Mao H, et al. Serum proteomics analysis reveals the thermal fitness of crossbred dairy buffalo to chronic heat stress[J]. *J Therm Biol*, 2020, 89: 102547.
13. Sun X, Qu T, He X, et al. Screening of differentially expressed proteins from syncytiotrophoblast for severe early-onset preeclampsia in women with gestational diabetes mellitus using tandem mass tag quantitative proteomics[J]. *BMC Pregnancy Childbirth*, 2018, 18(1): 437.
14. Budai Z, Balogh L, Sarang Z. Short-term high-fat meal intake alters the expression of circadian clock-, inflammation-, and oxidative stress-related genes in human skeletal muscle[J]. *Int J Food Sci Nutr*, 2019, 70(6): 749–758.
15. Park J C, Jeong W J, Seo S H, et al. WDR76 mediates obesity and hepatic steatosis via HRas destabilization[J]. *Sci Rep*, 2019, 9(1): 19676.
16. He F, Liu H, Guo X, et al. Direct Exosome Quantification via Bivalent-Cholesterol-Labeled DNA Anchor for Signal Amplification[J]. *Anal Chem*, 2017, 89(23): 12968–12975.
17. Xu X, Lai Y, Hua Z C. Apoptosis and apoptotic body: disease message and therapeutic target potentials[J]. *Biosci Rep*, 2019, 39(1).
18. Estornes Y, Toscano F, Virard F, et al. dsRNA induces apoptosis through an atypical death complex associating TLR3 to caspase-8[J]. *Cell Death Differ*, 2012, 19(9): 1482–94.
19. Shimokawa H, Sunamura S, Satoh K. RhoA/Rho-Kinase in the Cardiovascular System[J]. *Circ Res*, 2016, 118(2): 352–66.
20. Noma K, Oyama N, Liao J K. Physiological role of ROCKs in the cardiovascular system[J]. *Am J Physiol Cell Physiol*, 2006, 290(3): C661-8.
21. Ongusaha P P, Qi H H, Raj L, et al. Identification of ROCK1 as an upstream activator of the JIP-3 to JNK signaling axis in response to UVB damage[J]. *Sci Signal*, 2008, 1(47): ra14.
22. Cuzzocrea S, Mazzon E, Dugo L, et al. A role for superoxide in gentamicin-mediated nephropathy in rats[J]. *Eur J Pharmacol*, 2002, 450(1): 67–76.
23. Gong X, Celsi G, Carlsson K, et al. Protective effects of N-acetylcysteine amide (NACA) on gentamicin-induced apoptosis in LLC-PK1 cells[J]. *Ren Fail*, 2012, 34(4): 487–94.
24. Gong X, Duan Y, Zheng J, et al. Nephroprotective Effects of N-Acetylcysteine Amide against Contrast-Induced Nephropathy through Upregulating Thioredoxin-1, Inhibiting ASK1/p38MAPK Pathway, and Suppressing Oxidative Stress and Apoptosis in Rats[J]. *Oxid Med Cell Longev*, 2016, 2016: 8715185.
25. Zhou Y, Wang H D, Zhou X M, et al. N-acetylcysteine amide provides neuroprotection via Nrf2-ARE pathway in a mouse model of traumatic brain injury[J]. *Drug Des Devel Ther*, 2018, 12: 4117–4127.
26. Bian L, Meng Y, Zhang M, et al. MRE11-RAD50-NBS1 complex alterations and DNA damage response: implications for cancer treatment[J]. *Mol Cancer*, 2019, 18(1): 169.
27. Gong W, Martin T A, Sanders A J, et al. Location, function and role of stromal cell-derived factors and possible implications in cancer (Review)[J]. *Int J Mol Med*, 2021, 47(2): 435–443.
28. Inohara N, Koseki T, Del Peso L, et al. Nod1, an Apaf-1-like activator of caspase-9 and nuclear factor-kappaB[J]. *J Biol Chem*, 1999, 274(21): 14560–7.

29. Ahn B Y, Trinh D L, Zajchowski L D, et al. Tid1 is a new regulator of p53 mitochondrial translocation and apoptosis in cancer[J]. *Oncogene*, 2010, 29(8): 1155–66.
30. Zhang X, Su Y, Lin H, et al. The impacts of ubiquilin 1 (UBQLN1) knockdown on cells viability, proliferation, and apoptosis are mediated by p53 in A549 lung cancer cells[J]. *J Thorac Dis*, 2020, 12(10): 5887–5895.
31. Lu M, Ge Q, Wang G, et al. CIRBP is a novel oncogene in human bladder cancer inducing expression of HIF-1alpha[J]. *Cell Death Dis*, 2018, 9(10): 1046.
32. O'gorman D B, Costello M, Weiss J, et al. Decreased insulin-like growth factor-II/mannose 6-phosphate receptor expression enhances tumorigenicity in JEG-3 cells[J]. *Cancer Res*, 1999, 59(22): 5692–4.
33. Kusakabe M, Watanabe K, Emoto N, et al. Impact of DNA demethylation of the G0S2 gene on the transcription of G0S2 in squamous lung cancer cell lines with or without nuclear receptor agonists[J]. *Biochem Biophys Res Commun*, 2009, 390(4): 1283–7.
34. Chen X, Gu P, Xie R, et al. Heterogeneous nuclear ribonucleoprotein K is associated with poor prognosis and regulates proliferation and apoptosis in bladder cancer[J]. *J Cell Mol Med*, 2017, 21(7): 1266–1279.
35. Liu H, Ma Y, He H W, et al. SLC9A3R1 stimulates autophagy via BECN1 stabilization in breast cancer cells[J]. *Autophagy*, 2015, 11(12): 2323–34.
36. Shi L, Al-Baadani A, Zhou K, et al. PCMT1 Ameliorates Neuronal Apoptosis by Inhibiting the Activation of MST1 after Subarachnoid Hemorrhage in Rats[J]. *Transl Stroke Res*, 2017.
37. Zhu Z, Wang S, Cao Q, et al. CircUBQLN1 Promotes Proliferation but Inhibits Apoptosis and Oxidative Stress of Hippocampal Neurons in Epilepsy via the miR-155-Mediated SOX7 Upregulation[J]. *J Mol Neurosci*, 2021, 71(9): 1933–1943.
38. Fang X, Wang H, Han D, et al. Ferroptosis as a target for protection against cardiomyopathy[J]. *Proc Natl Acad Sci U S A*, 2019, 116(7): 2672–2680.

Figures

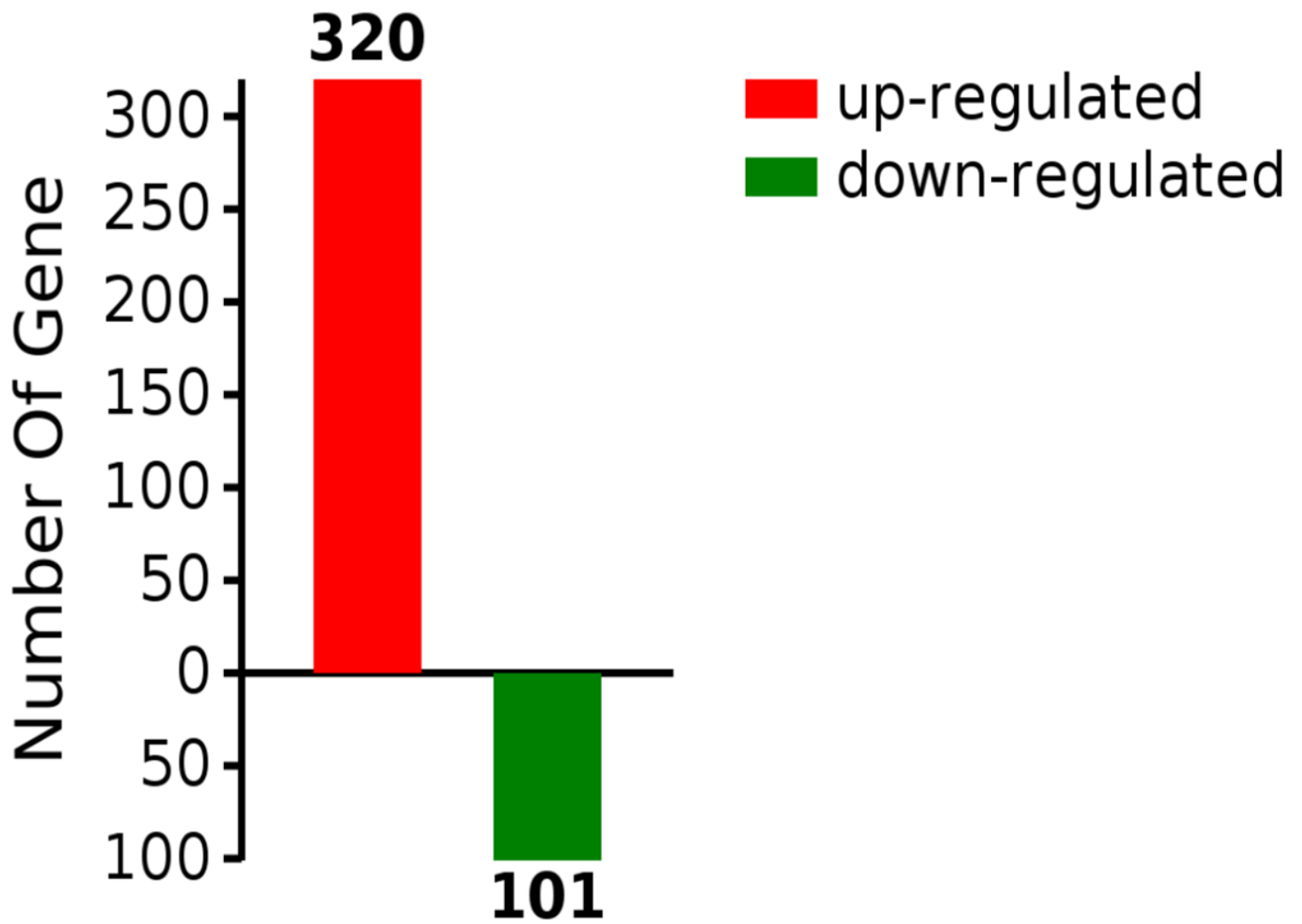


Figure 1

Hepatic proteomic changes in mice after G0S2 overexpression.

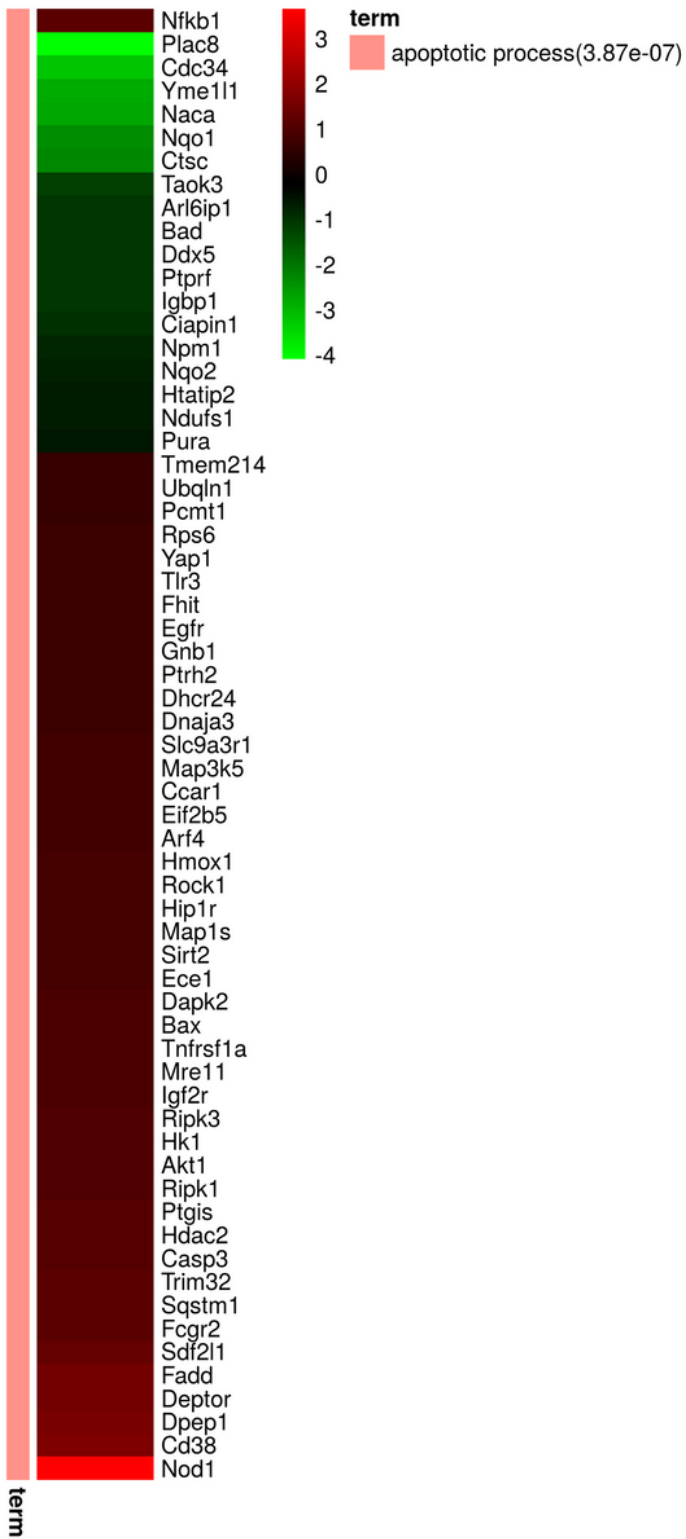


Figure 2

Heatmap of 63 differentially expressed proteins in apoptotic process.

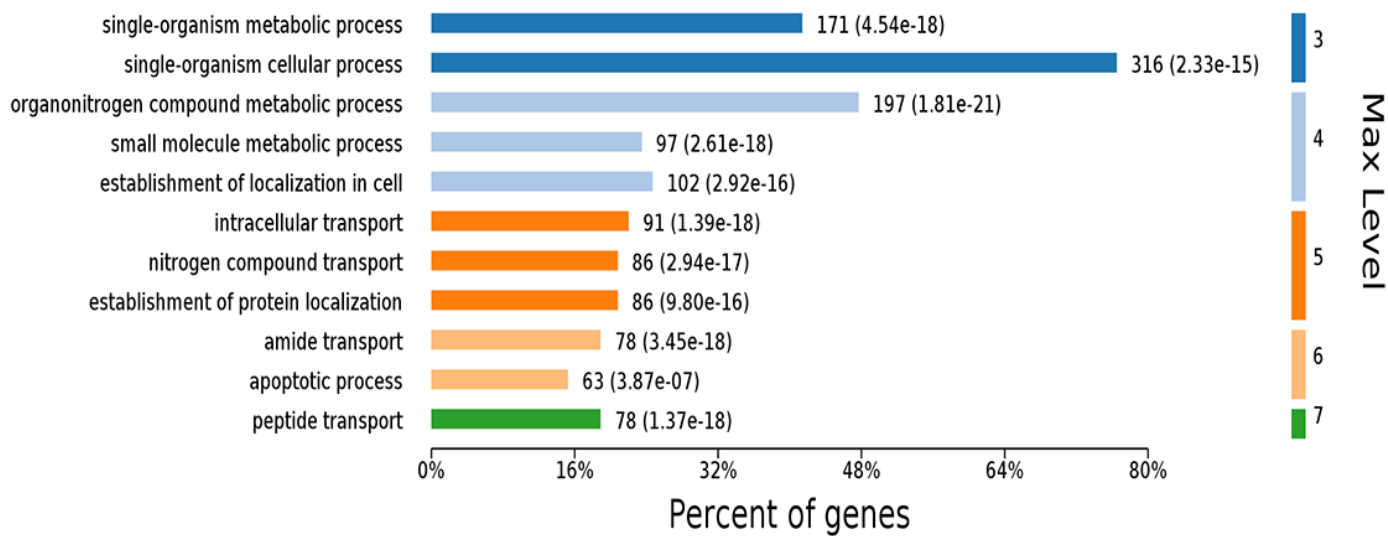


Figure 3

GO analysis of biological process of 421 identified differential proteins.

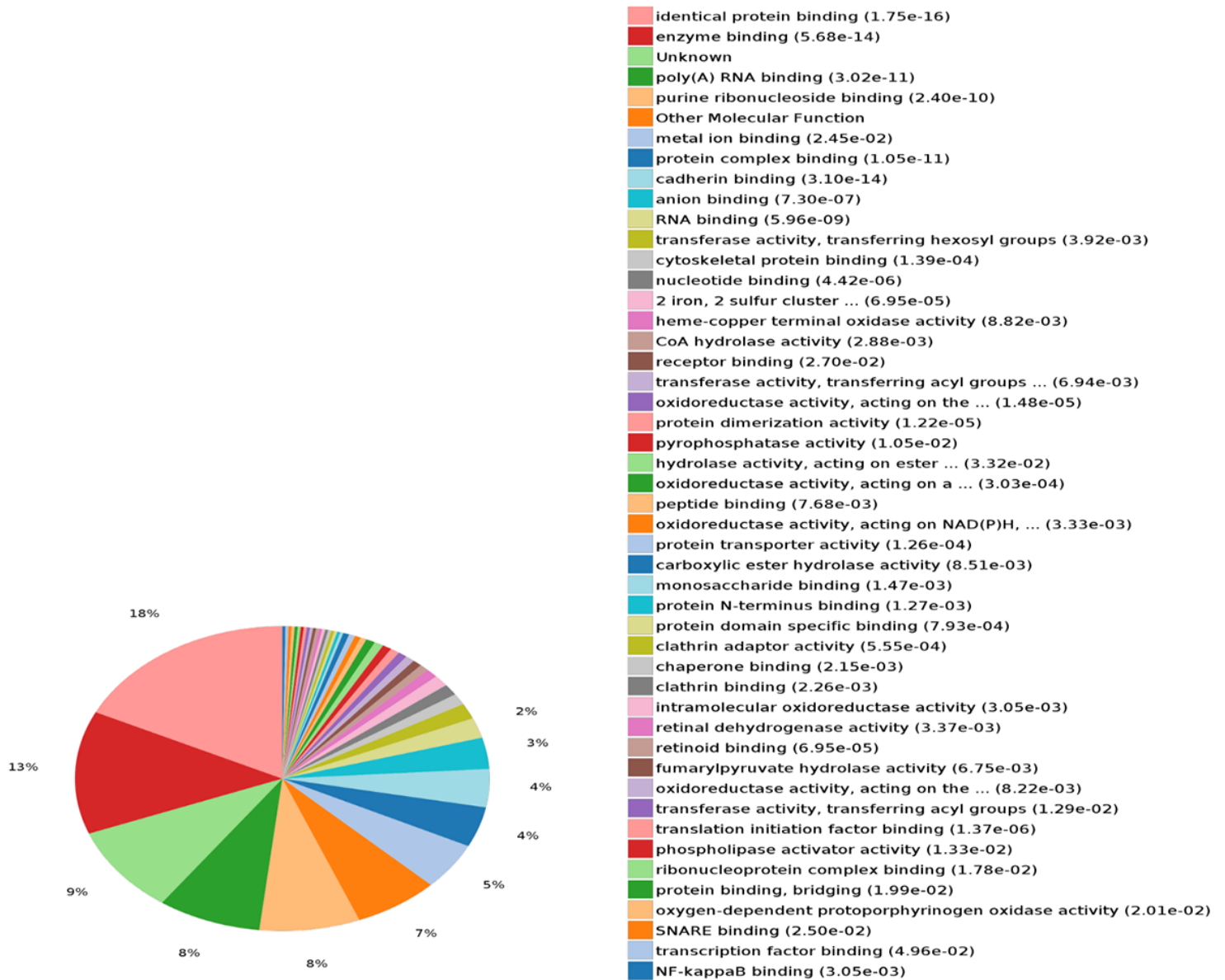


Figure 4

GO analysis of molecular function of 421 identified differential proteins.

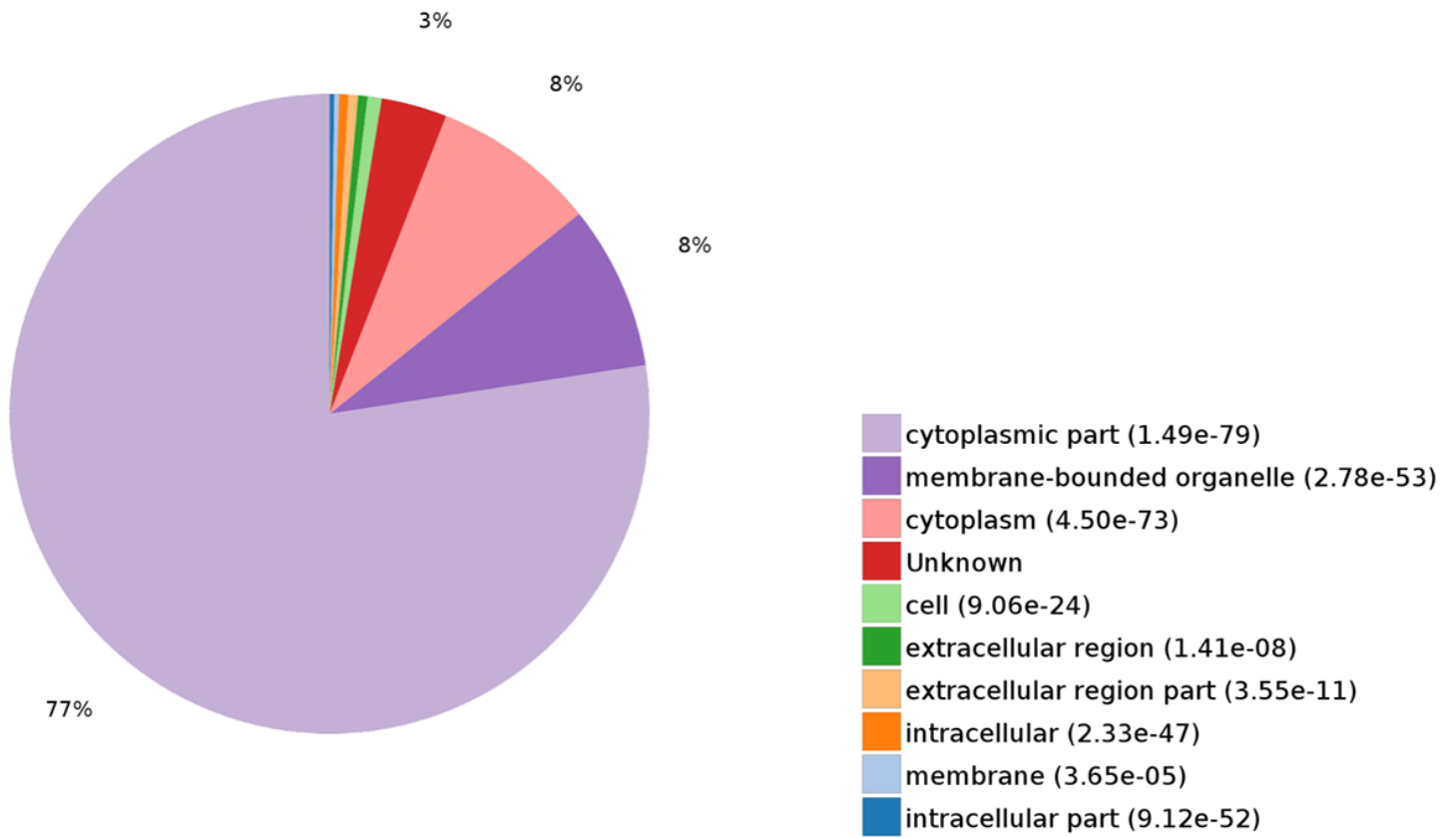


Figure 5

GO analysis of cellular components of 421 identified differential proteins.

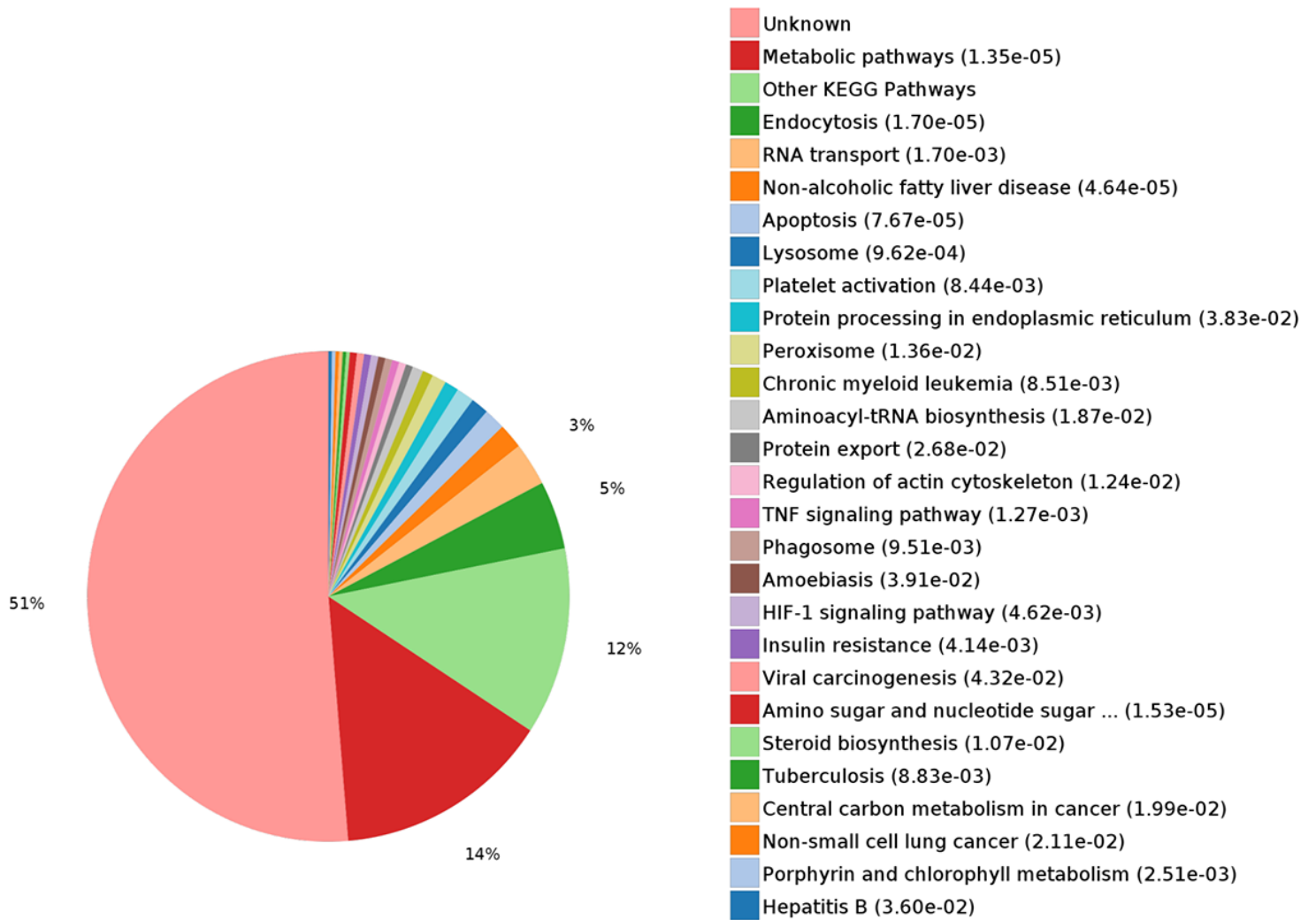


Figure 6

KEGG pathway analysis of differentially expressed proteins involved in various biological signaling pathways.

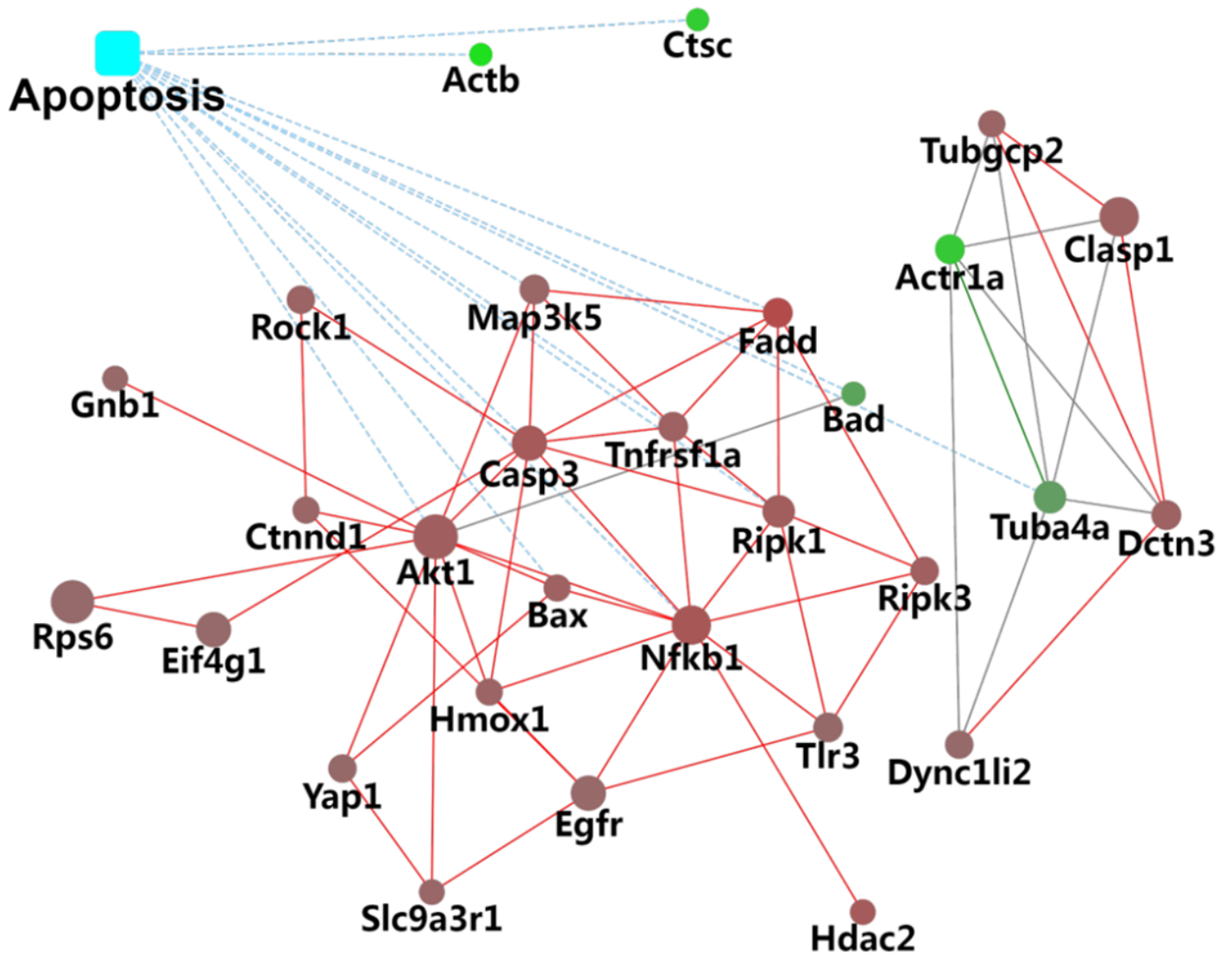


Figure 7

Protein-protein interaction (PPI) network analysis of differentially apoptosis-associated proteins.

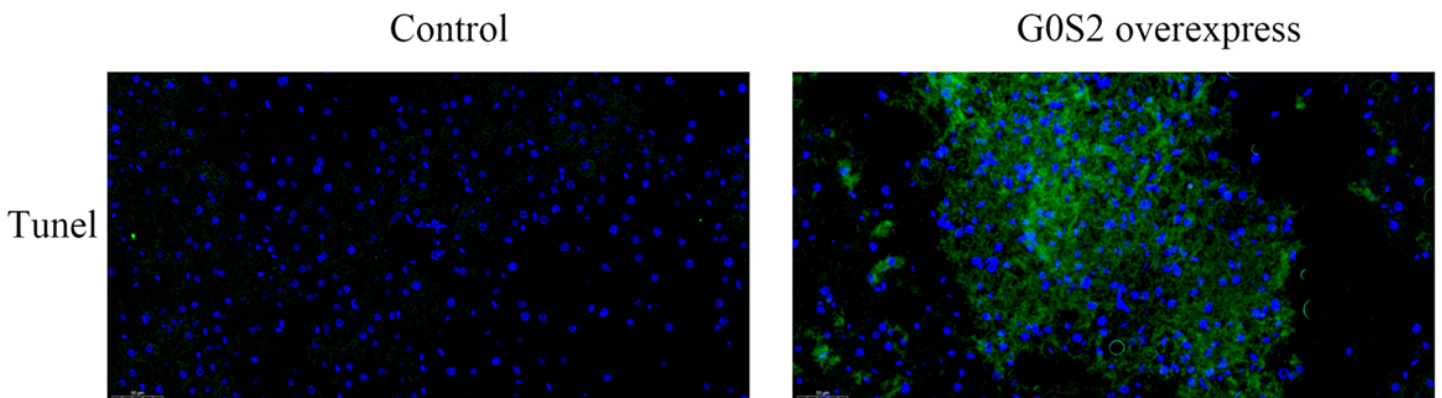


Figure 8

TUNEL staining shows apoptosis in liver cells.

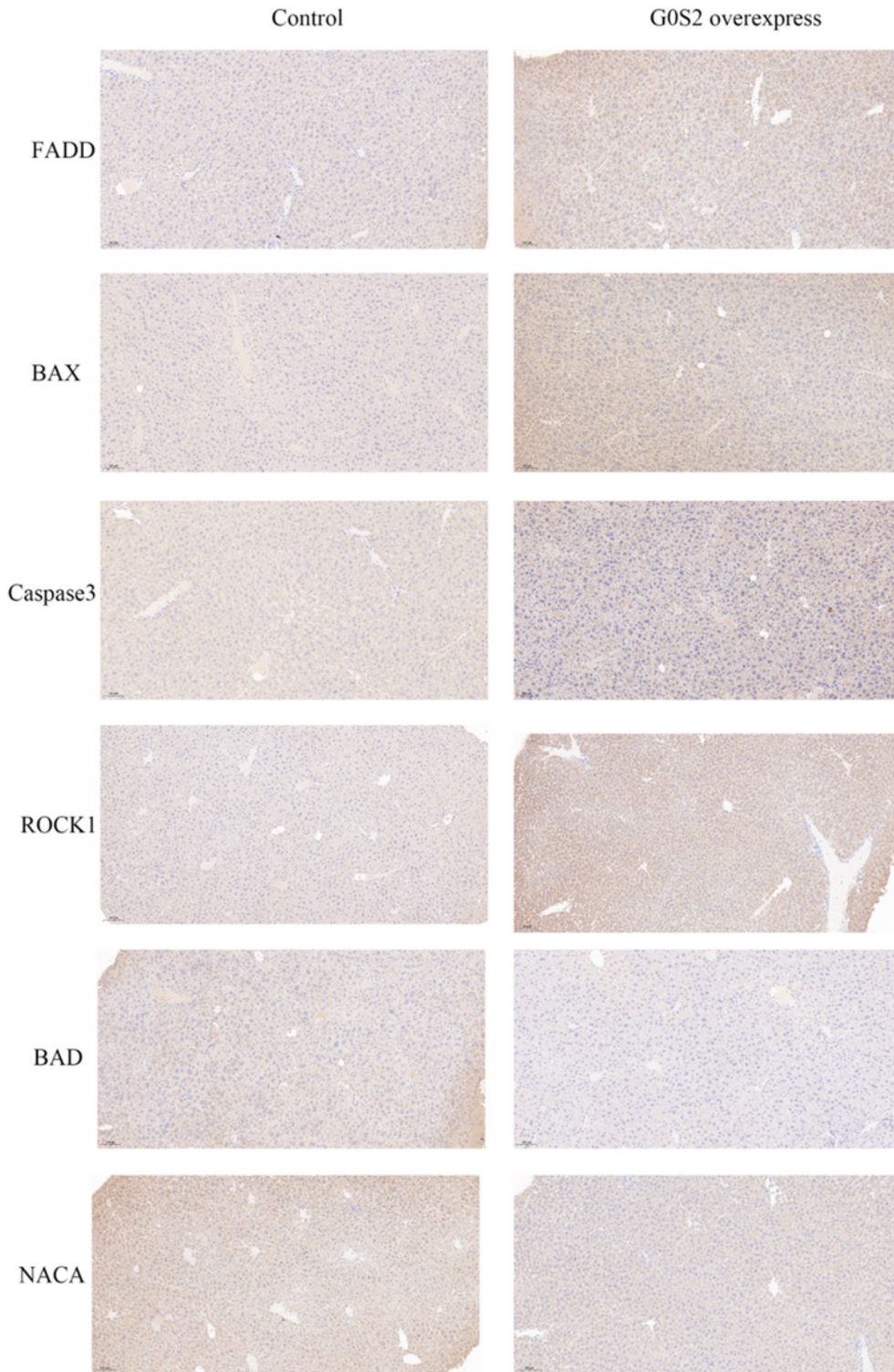


Figure 9

Immunohistochemical assays for the expression of FADD, BAX, Caspase3, ROCK1, BAD, NACA.

Supplementary Files

This is a list of supplementary files associated with this preprint. Click to download.

- [proteomicssupplementaryfile.xlsx](#)